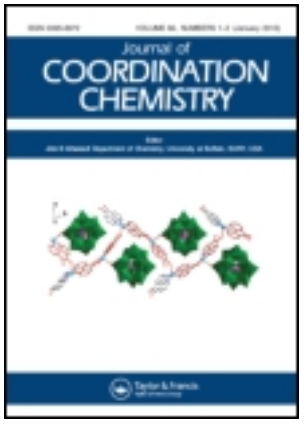

Journal of Coordination Chemistry
Publication details, including instructions for authors and subscription information:
http://www.tandfonline.com/loi/gcoo20

Synthesis, crystal structure, and bioactivity of two triphenylantimony derivatives with benzohydroxamic acid and N-phenylbenzohydroxamic acid

Qingkun Wu [a], Handong Yin [a], Caihong Yue [a], Xiuyun Zhang [a], Min Hong [a] & Jichun Cui [a]

[a] Shandong Provincial Key Laboratory of Chemical Energy Storage and Novel Cell Technology, School of Chemistry and Chemical Engineering, Liaocheng University, Liaocheng 252059, P.R. China

Published online: 15 May 2012.

To cite this article: Qingkun Wu, Handong Yin, Caihong Yue, Xiuyun Zhang, Min Hong & Jichun Cui (2012) Synthesis, crystal structure, and bioactivity of two triphenylantimony derivatives with benzohydroxamic acid and N-phenylbenzohydroxamic acid, Journal of Coordination Chemistry, 65:12, 2098-2109, DOI: 10.1080/00958972.2012.688118

To link to this article: http://dx.doi.org/10.1080/00958972.2012.688118

Journal of Coordination Chemistry
Vol. 65, No. 12, 20 June 2012, 2098–2109

Synthesis, crystal structure, and bioactivity of two triphenylantimony derivatives with benzohydroxamic acid and *N*-phenylbenzohydroxamic acid

QINGKUN WU, HANDONG YIN*, CAIHONG YUE, XIUYUN ZHANG, MIN HONG and JICHUN CUI

Shandong Provincial Key Laboratory of Chemical Energy Storage and Novel Cell Technology, School of Chemistry and Chemical Engineering, Liaocheng University, Liaocheng 252059, P.R. China

(*Received 5 November 2011; in final form 14 March 2012*)

Reaction of triphenylantimony dichloride with benzohydroxamic acid or *N*-phenylbenzohydroxamic acid in 1 : 1 stoichiometry yielded two new triphenylantimony derivatives formulated as $[Ph_3SbL_1L_2]$ (L_1 = benzohydroxamato, L_2 = methoxide, **1**; L_1 = N-phenylbenzohydroxamato, L_2 = Cl, **2**), which have been characterized by FT-IR, NMR spectroscopy, elemental analysis, and melting point. Single-crystal X-ray diffraction analyses for **1** and **2** reveal that the antimony is six-coordinate adopting distorted octahedral geometry with one phenyl and methoxide or chloride in axial positions. In the supramolecular structure, a double-chain is shown for **2** constructed by C–H $\cdots$ X (X = O, C or π) weak interactions, while **1** exhibits a 1-D-chain structure connected by O–H $\cdots$ O and N–H $\cdots$ N hydrogen bonds. *In vitro* antitumor study reveals that **1** and **2** display activities against two human tumor cell lines – A549 and HCT-8. To explore the antitumor activity mechanism, DNA binding properties of **1** and **2** with calf thymus DNA (*ct*-DNA) have been investigated by fluorescence spectra, indicating that **1** and **2** bind to *ct*-DNA *via* intercalation, which could induce the death of cancer cells.

Keywords: Organoantimony(V) complex; Hydroxamic acid; Structure analysis; DNA-EB; Antitumor

1. Introduction

Attention has been directed to the chemistry of organoantimony(V) due to structure diversity (from monomeric molecular species, associated structures, and supramolecular assemblies [1, 2]) as well as its applications as antimicrobial [3–6] and antitumor agent [7, 8], which was reviewed by Tiekink [9]. There are a number of references describing the synthesis and applications of $Ar_nSbX_{(5-n)}$ ($n = 3$, 4; X = oximate, carboxylate, halide, alkoxyl, sulphonate) [10–14], but to the best of our knowledge, reports on organoantimony derivatives from hydroxamic acids are limited, although organotin complexes derived from hydroxamic aicds are of current interest [15, 16]. As a result of their tautomerization and potential as therapeutics, hydroxamic acids have been widely

*Corresponding author. Email: handongyin@163.com

ISSN 0095-8972 print/ISSN 1029-0389 online © 2012 Taylor & Francis
http://dx.doi.org/10.1080/00958972.2012.688118

researched in organometallic chemistry and biochemistry [17–19]. Progress has been summarized by three classical reviews [20–22].

Li and coworkers have synthesized several organoantimony arylhydroxamates and have reported their *in vitro* bioactivity against several human tumor cell lines [23]. As an extension of this field, we chose two arylhydroxamic acids as a supporting ligand to construct new organoantimony derivatives and two six-coordinate triphenylantimony complexes have been obtained. As preliminary exploration of their bioactivity, *in vitro* antitumor activity has been tested against two human tumor cell lines – A549 and HCT-8 [24, 25]. Although DNA-binding abilities have been used to research the bioactivity of some transition and main-group metal derivatives, there is no report focusing on the DNA-binding of organoantimony compounds. Herein, to explore the mechanism of antitumor activity, DNA-binding properties of the two compounds with calf thymus DNA (*ct*-DNA) have also been investigated by fluorescence spectra [26]. Our investigation demonstrates that the antitumor activity of the title complexes may be due to the interaction between organoantimony compounds and DNA, which can bring DNA damage in cancer cells, blocking the division of cancer cells and resulting in cell death.

2. Experimental details

2.1. *Synthesis of the title compounds*

2.1.1. $[(C_6H_5)C(O)NHOSb(C_6H_5)_3(CH_3O)] \cdot 0.5CH_2Cl_2$ (1). The reaction was carried out under nitrogen by standard Schlenk techniques. Benzohydroxamic acid (44.8 mg, 0.4 mmol) and potassium hydroxide (22.4 mg, 0.4 mmol) were dissolved in 40 mL solution of methanol and toluene (1:1) and stirred for 0.5 h. Then triphenylantimony dichloride (169.6 mg, 0.4 mmol) was added to the mixture and the reaction continued for 8 h at room temperature. After filtration, solvents were evaporated *in vacuo*. The obtained solid was recrystallized from dichloromethane:methanol (1:1). Yield: 76%. m.p. 139–141°C. Anal. Calcd for $C_{26}H_{24}NO_3Sb$ (%): C, 60.03; H, 4.65; N, 2.69. Found (%): C, 60.36; H, 4.82; N, 2.48. IR (KBr, cm^{-1}): 1635 (w, C=O); 694 (s, N–O); 461 (s, Sb–C); 416 (m, Sb–O). ^1H NMR ($CDCl_3$, 400 MHz, ppm): $\delta = 7.97$ [b, 2H, Ph(–C=O)–H]; 7.75 [m, 3H, Ph(–C=O)–H]; 7.37–7.53 [m, 15H, Ph(–Sb)–H]; 5.29 (s, 1H, CH_2Cl_2); 3.46 (s, 3H, CH_3); 1.90 (s, 1H, N–H). ^{13}C NMR ($CDCl_3$, 101 MHz, ppm): $\delta = 162.27$ (C=O); 125–137 (Ph–C); 53.63 (CH_2Cl_2); 51.00 (CH_3).

2.1.2. $[(C_6H_5)C(O)N(C_6H_5)OSb(C_6H_5)_3 \cdot Cl]$ (2). The preparation procedure was the same as **1**. The yellow solid was recrystallized from petroleum ether:ethyl ether (1 : 1) to give yellow crystals. Yield: 65%, m.p. 150–152°C. Anal. Calcd for $C_{31}H_{25}ClNO_2Sb$ (%): C, 61.98; H, 4.19; N, 2.33. Found (%): C, 61.62; H, 4.36; N, 2.48. IR (KBr, cm^{-1}): 1638 (m, C=O); 694 (s, N–O); 462 (m, Sb–C); 438 (s, Sb–O). ^1H NMR ($CDCl_3$, 400 MHz, ppm): $\delta = 7.03$–7.53 [m, 15H, Ph(–Sb)–H]; 7.54–7.92 [m, 5H, Ph(–NC(=O))–H]; 7.92–8.31 [m, 5H, Ph(C=O–H]. ^{13}C NMR ($CDCl_3$, 101 MHz, ppm): 163.25, (C=O); 146.98, (–N–O); 146.33, [–C(=O)–N]; 122.61–143.58, (Ph–C).

2.2. *X-ray crystallography*

Diffraction data for **1** and **2** were obtained on a Bruker Smart 1000 CCD diffractometer (graphite monochromated Mo-Kα radiation, $\lambda = 0.71073$ Å). All data were corrected using SADABS and the final refinement was performed by full-matrix least-squares with anisotropic thermal parameters for non-hydrogen atoms on F^2 using SHELX-97. The hydrogen atoms were added theoretically, riding on the concerned atoms and refined with fixed thermal factors.

2.3. *Fluorescence spectra*

ct-DNA and ethidium bromide (EB) were dissolved in 10 mmol L^{-1} trihydroxymethylaminomethane (tris)-HCl buffer solution and the *ct*-DNA concentration per nucleotide was determined by absorption spectroscopy using the molar absorption coefficient (6600 L mol^{-1} cm^{-1}) at 260 nm, while the EB concentration was calculated by the ratio of the mass to its molecular weight. The title compounds were dissolved in methanol and the concentration was determined in the same way as EB. The organoantimony complexes were added to the solution containing 30 μmol L^{-1} *ct*-DNA and 3 μmol L^{-1} EB at different concentrations (0–180 μmol L^{-1}). After 2 h, fluorescence quenching spectra were recorded at 530–700 nm with all samples excited at 258 nm.

2.4. In vitro *antitumor activity*

Two cell lines, human lung cancer cell line (A549) and human colon cell line (HCT-8), were used for screening. They were maintained in the logarithmic phase in 37°C in 5% carbon dioxide atmosphere using culture media containing 10% fetal calf serum and 1% antibiotics (50 units mL^{-1} penicillin and 50 μg mL^{-1} streptomycin): RPMI-1640 medium for HCT-8 and D-MEM medium for A549. Cell proliferation in the compound-treated culture was evaluated by the MTT (tetrazolium salt reduction) assay. Briefly, cells were seeded in 96-well micro-plates in growth medium (100 μL) and then incubated at 37°C in 5% carbon dioxide atmosphere. After 24 h, the medium was removed and replaced by fresh media, including the compound to be studied at an appropriate concentration. The compound solution was diluted serially with DMSO; 48 h later, each well was treated with 10 μL of 5 mg mL^{-1} MTT [3-(4,5dimethylthiazol-2-yl)-2,5-diphenyltetrazolium bromide] saline solution and after another 4 h of incubation, the culture medium was replaced by 100 μL DMSO to resolve the insoluble blue formazan precipitates produced by MTT reduction. The plates were shaken for 20 min to ensure complete dissolution and then inhibition of the cell growth induced by the tested compound was detected by measuring the absorbance of each well at 570 nm.

3. Results and discussion

3.1. *Preparations*

Compounds **1** and **2** are prepared under dry nitrogen using Schlenk techniques and both of them are stable at ambient conditions. They are soluble in common organic

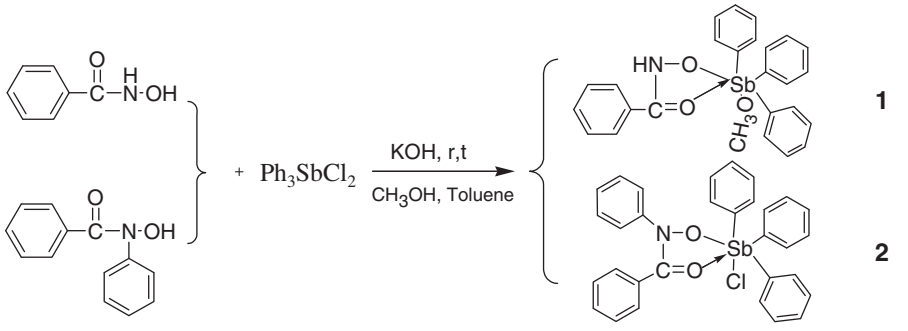

Scheme 1. The reaction procedures.

solvents, such as chloroform, acetone, methanol, and dimethylsulfoxide, but insoluble in hexane, ether, and petroleum ether. The synthesis procedure of **1** and **2** is given in scheme 1.

3.2. *IR spectra*

Infrared (IR) spectra of **1** and **2** were recorded from 400 to 4000 cm^{-1} and the absorptions were assigned on the basis of earlier literature [27]. By comparing IR spectra of complexes with free ligands, complete disappearance of the stretching vibration of O–H indicates the coordination of hydroxyl oxygen to antimony with associated Sb–O absorptions (416 and 438 cm^{-1}) in the range reported for other organoantimony complexes. When there are interactions between antimony and carbonyl oxygen from the hydroxamato, the absorption values of C=O decreased, as observed for **1** and **2** (1635 and 1638 cm^{-1}, respectively). The absorptions of Sb–C are 462 and 461, respectively, which are consistent with previous publications [23, 27].

3.3. *NMR spectra*

In ^{1}H NMR spectra, protons of phenyls bound to antimony shift to high-field while protons of phenyls in ligands to low-field [28]. The signal of –OH is absent, indicating the removal of the hydroxyl proton and the formation of Sb–O bond, consistent with IR data. For **1**, 5.46 ppm suggests solvent CH_2Cl_2 and the singlet at 3.29 can be assigned to $–CH_3$ of methoxide. In ^{13}C-NMR spectra, peaks at 51.00 and 53.68 ppm can be attributed to $–CH_3$ and CH_2Cl_2, respectively. The two derivatives also exhibit signals ascribed to carbons of aryl at 122–143 ppm.

3.4. *Crystal structure*

Crystals of **1** $0.5CH_2Cl_2$, suitable for the X-ray crystallographic study were grown from dichloromethane and methanol, whilst crystals of **2** suitable for the X-ray crystallographic study were obtained from the mixture of dichloromethane and petroleum ether.

Table 1. Crystal data and structure refinement parameters for **1** and **2**.

Complex	**1**	**2**
Empirical formula	$C_{53}H_{48}Cl_2N_2O_6Sb_2$	$C_{31}H_{25}ClNO_2Sb$
Formula weight	1123.33	600.72
Wavelength (Å)	0.71073	0.71073
Crystal system	Monoclinic	Triclinic
Space group	$C2/c$	$P\bar{1}$
Unit cell dimensions (Å, °)		
a	30.011(3)	9.4567(11)
b	11.2156(12)	10.1597(13)
c	17.6317(16)	14.9704(16)
α	90	93.5600(10)
β	124.6300(10)	101.7380(10)
γ	90	105.000(2)
Volume (Å^3), Z	4883.3(8), 4	1350.2(3), 2
Calculated density (Mg m^{-3})	1.528	1.478
Absorption coefficient (mm^{-1})	1.267	1.149
$F(000)$	2256	604
Crystal size (mm^3)	$0.38 \times 0.31 \times 0.31$	$0.45 \times 0.38 \times 0.22$
Reflections collected	11,952	7010
Independent reflection	4300 [R(int) = 0.0251]	4681 [R(int) = 0.0161]
Data/restraints/parameters	4300/0/301	4681/2/325
Goodness-of-fit on F^2	1.607	1.061
Final R indices [$I > 2\sigma$ (I)]	$R_1 = 0.0820$, $wR_2 = 0.1976$	$R_1 = 0.0287$, $wR_2 = 0.0695$
R indices (all data)	$R_1 = 0.0875$, $wR_2 = 0.2000$	$R_1 = 0.0356$, $wR_2 = 0.0748$

The most relevant crystallographic data for **1** $0.5CH_2Cl_2$ and **2** are summarized in table 1, while selected bond lengths and angles are shown in table 2.

The reaction between benzohydroxamic acid and triphenylanimony dibromide has been carried out by Li *et al*. and the crystal structure of $[Ph_3SbL_2]^-$ $[HNEt_3]^+$ has been reported [23]. To construct various conformations and to further investigate the role of the supporting ligand, we launched a similar reaction and a new organoantimony derivative was obtained, as shown in figure 1. Antimony has a coordination number of six (figure 1), binding to three phenyl groups, one methoxide, and two oxygen atoms from benzohydroxamato in a distorted octahedron. Antimony–oxygen bond lengths in organoantimony compounds are extremely variable [29], ranging from 1.925 Å in $(Ph_3SbO)_2$ [30] to 2.506 Å in Ph_4SbOSO_2Ph [31] and the Sb(1)–O(2), Sb(1)–O(3), and Sb(1)–O(4) distances [2.223(8), 2.104(7), and 2.081(7) Å, respectively] in **1** all lie within this range. There is no significant difference between Sb(1)–O(3) and Sb(1)–O(4) bond lengths, indicating the benzohydroxamic acid coordinates to the antimony in a O, O bidentate mode. Sb(1)–O(2) distance, 2.223(8) Å, shows that the interaction between methoxide and antimony center is also strong. The four atoms occupying the equatorial positions O(3), O(4), C(8), and C(14) are coplanar within 0.0185(46) Å and the deviation of Sb from this plane is just 0.1600(51) Å leaning to C20.

$[Ph_3Sb(bhaMeO)]$ (bha = benzohydroxamato) crystallizes with CH_2Cl_2, but no obvious interaction between them is observed and in figures 1 and 2 solvent molecules are omitted. In every adjacent two molecules, only one N(1) is deprotonated and as does O(2), thus hydrogen bond interactions O(2)–H···O(2) and N(1)–H···N(1) exist (table 3). Through the O(2)–H···O(2) hydrogen bond, two molecules bind together into a centro-symmetric (symmetric operation: $-x$, $-y$, $-z$) dimer (shown in figure 2a),

Table 2. Selected bond lengths (Å) and angles (°) for **1** and **2**.

1			
Sb(1)–O(4)	2.081(7)	O(4)–Sb(1)–C(14)	159.9(3)
Sb(1)–O(3)	2.104(7)	O(3)–Sb(1)–C(14)	86.0(4)
Sb(1)–C(8)	2.111(12)	C(8)–Sb(1)–C(14)	104.5(4)
Sb(1)–C(14)	2.134(10)	O(4)–Sb(1)–C(20)	90.7(3)
Sb(1)–C(20)	2.184(11)	O(3)–Sb(1)–C(20)	90.6(4)
Sb(1)–O(2)	2.223(8)	C(8)–Sb(1)–C(20)	98.6(4)
N(1)–C(7)	1.298(13)	C(14)–Sb(1)–C(20)	95.7(4)
N(1)–O(4)	1.389(11)	O(4)–Sb(1)–O(2)	83.9(3)
O(3)–C(7)	1.305(12)	O(3)–Sb(1)–O(2)	81.7(3)
O(4)–Sb(1)–O(3)	74.9(3)	C(8)–Sb(1)–O(2)	88.3(4)
O(4)–Sb(1)–C(8)	93.3(3)	C(14)–Sb(1)–O(2)	87.4(3)
O(3)–Sb(1)–C(8)	165.1(4)	C(20)–Sb(1)–O(2)	171.5(4)
2			
Sb(1)–C(14)	2.133(3)	C(14)–Sb(1)–C(20)	99.16(12)
Sb(1)–O(2)	2.137(2)	O(2)–Sb(1)–C(20)	88.52(10)
Sb(1)–C(26)	2.141(3)	C(26)–Sb(1)–C(20)	97.70(12)
Sb(1)–C(20)	2.155(3)	C(14)–Sb(1)–O(1)	90.47(10)
Sb(1)–O(1)	2.155(2)	O(2)–Sb(1)–O(1)	72.77(8)
Sb(1)–Cl(1)	2.5094(10)	C(26)–Sb(1)–O(1)	163.41(10)
N(1)–C(1)	1.299(4)	C(20)–Sb(1)–O(1)	86.63(10)
N(1)–O(1)	1.347(3)	C(14)–Sb(1)–Cl(1)	88.70(9)
O(2)–C(1)	1.323(3)	O(2)–Sb(1)–Cl(1)	80.59(7)
C(14)–Sb(1)–O(2)	161.20(11)	C(26)–Sb(1)–Cl(1)	91.73(10)
C(14)–Sb(1)–C(26)	104.54(12)	C(20)–Sb(1)–Cl(1)	165.76(8)
O(2)–Sb(1)–C(26)	91.27(10)	O(1)–Sb(1)–Cl(1)	81.42(6)

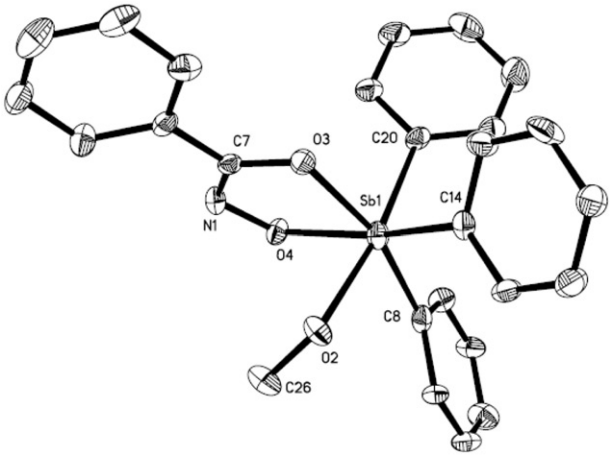

Figure 1. The molecular structure of **1** (the uncoordinated solvent molecule and hydrogen atoms have been omitted for clarity).

which extends along the *c* axis by the N(1)–H $\cdots$ N(1) hydrogen bond into a 1-D zigzag chain structure (figure 2b).

A perspective view of **2** is shown in figure 3 and it is similar to **1**. The antimony also exhibits six-coordinate distorted octahedral geometry, binding with three phenyl groups

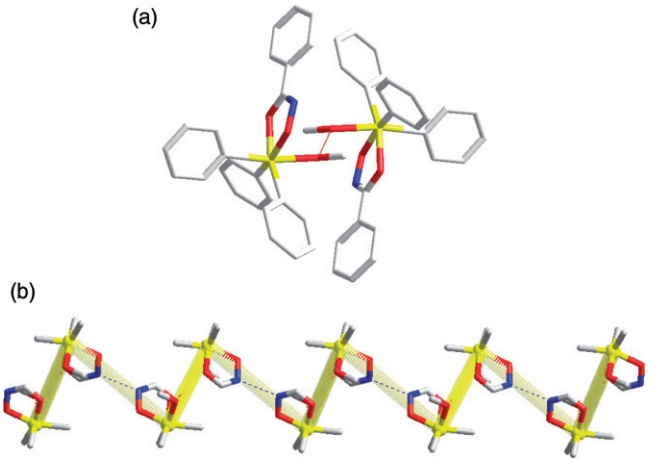

Figure 2. (a) The dimer of **1**; (b) 1-D zigzag chain structure of **1**.

Table 3. Hydrogen bonding geometries for **1**.

D–H···A	H···A (Å)	D···A (Å)	D–H···A (°)
O(2)–H(2A)···O(2)#1	1.90	2.643(15)	151.1
N(1)–H(1)···N(1)#2	2.05	2.866(17)	157.8

Symmetry code: #1: $-x, -y, -z$; #2: $-x, y, -z-1/2$.

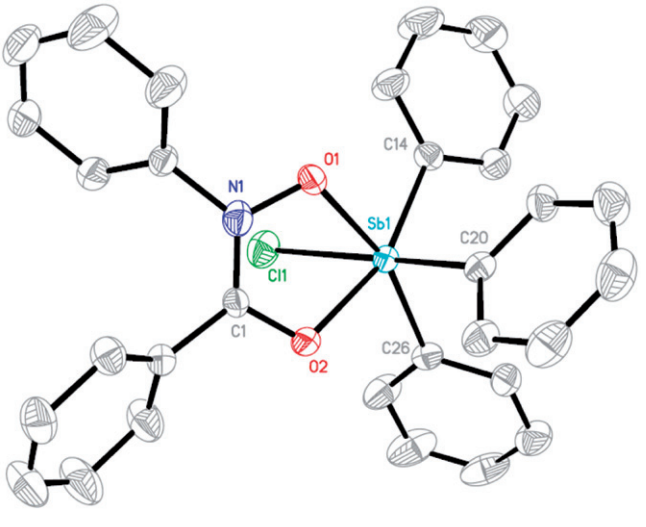

Figure 3. The molecular structure of **2**.

and the bidentate deprotonated organic ligand. The four equatorial atoms, O(1), O(2), C(14), and C(26), are almost coplanar with an average deviation of 0.0320(14) Å and the antimony is 0.1406 Å from this plane leaning to C(20). Compared with **1** the methoxide group is replaced by a chloride, which may be ascribed to the steric effect of

Table 4. C–H···O, C–H···C, and C–H···π weak hydrogen bonds of **2**.

	C–H (Å)	H–X (Å)	C–X (Å)	C–H···X (°)
C16–H16···O2#1	0.929	2.714	3.544	149.16
C10–H10···C15#2	0.930	2.875	3.686	146.53
C17–H17···π (centroid)#1	0.930	2.637	3.536	154.83

Symmetry code: #1: $x-1$, y, z; #2: $-x+1$, $-y+2$, $-z+2$.

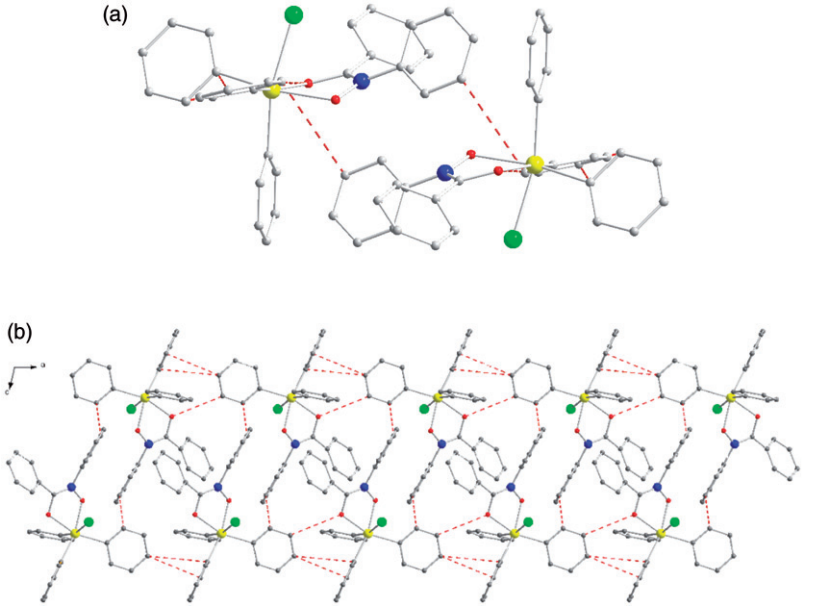

Figure 4. The double-chain structure of **2** connected by C–H···X WHBs interaction: (a) view along the *a*-axis; (b) view along the *b*-axis.

two phenyl groups in *N*-phenylbenzohydroxamato. The bond lengths of Sb–O, Sb–C, and Sb–Cl are all consistent with those reported in the literature [23, 27]. Although, resembling benzohydroxamato in **1**, *N*-phenylbenzohydroxamato coordinates to antimony in an O,O bidentate mode, the bond length of Sb–O is a little longer (av. 0.054 Å), which can also be ascribed to steric hindrance of the *N*-phenyl group.

Analysis of the supramolecular structure of **2** reveals that it is different from **1** and intermolecular C–H···O, C–H···C and C–H···π weak hydrogen bonds (WHBs) play an important role in supramolecular assembly (table 4). The C–H···π WHBs can be viewed as an edge-to-face (as opposed to point-to-face or T-shape) π–π interaction [32, 33]. Although both are much weaker than covalent and coordinated interactions, and even than typical hydrogen bonds, they clearly govern the assembly of the molecules in many compounds [34]. As shown in figure 4, a series of parallel chains connected by intermolecular C(16)–H(16)···O(2) and C(17)–H(17)···π [C(26) to (C31)] double WHBs running along the *a*-axis have been found.

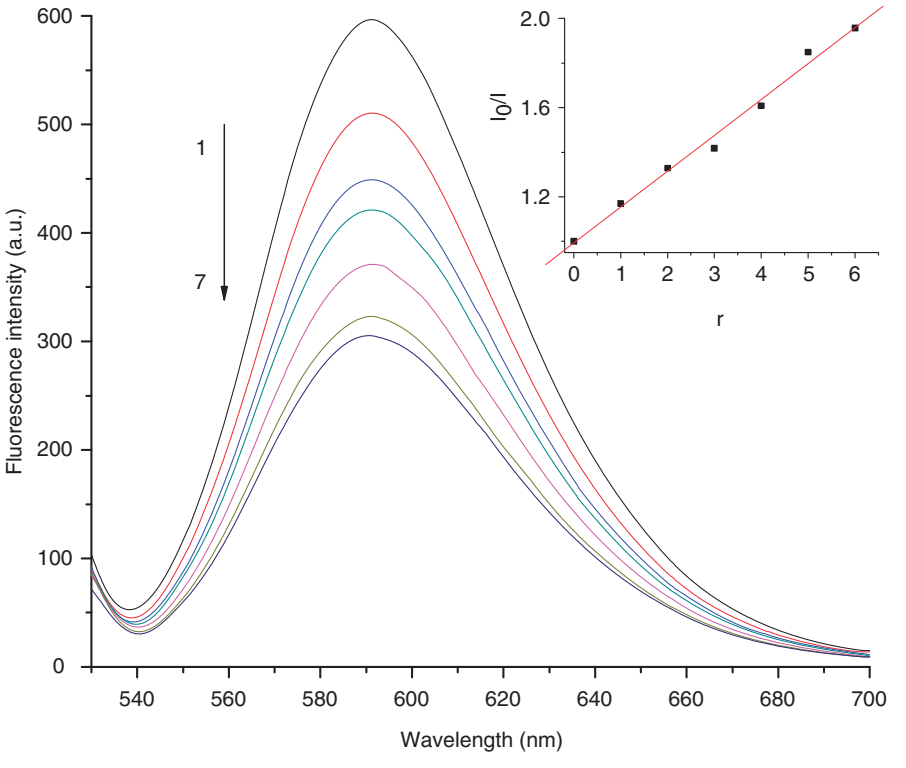

Figure 5. Effects of **1** on the fluorescence spectra of EB-DNA system. $C_{DNA} = 30\,\mu mol\,L^{-1}$; $C_{EB} = 3\,\mu mol\,L^{-1}$; from 1 to 7 $C_{VOL} = 0$, 30, 60, 90, 120, 150, 180 $\mu mol\,L^{-1}$, respectively; Inset: plot of I_0/I *vs.* r ($r = C_{VOL}/C_{DNA}$). $\lambda_{ex} = 258$ nm.

3.5. *Fluorescence spectra*

To investigate the interaction between DNA and **1** and **2**, EB was used as a probe. EB has weak fluorescence, but in the presence of DNA its emission intensity can be greatly enhanced because of its strong intercalation between adjacent DNA base pairs. This enhanced fluorescence can be quenched, at least partly, by the addition of another molecule [35]. Fluorescence quenching assays of EB bound to excess DNA is utilized to differentiate intercalative and non-intercalative molecules. The fluorescence quenching curves of EB bound to DNA by **1** and **2** are shown in figures 5 and 6. Addition of samples into DNA pretreated with EB causes appreciable reduction in the emission intensity, which indicates the replacement of EB by organoantimony complexes. Thus, the title compounds bind to DNA by intercalation. According to the classical Stern–Volmer equation:

$$I_0/I = 1 + K_{sq}r$$

where I_0 and I represent fluorescence intensities in the absence and presence of the samples, respectively; r corresponds to the concentration ratio of the sample to DNA. K_{sq}, the linear Stern–Volmer constant, can be obtained from the slope of I_0/I *versus* r linear plot; it depends on the concentration of EB bound to DNA. From the insets in

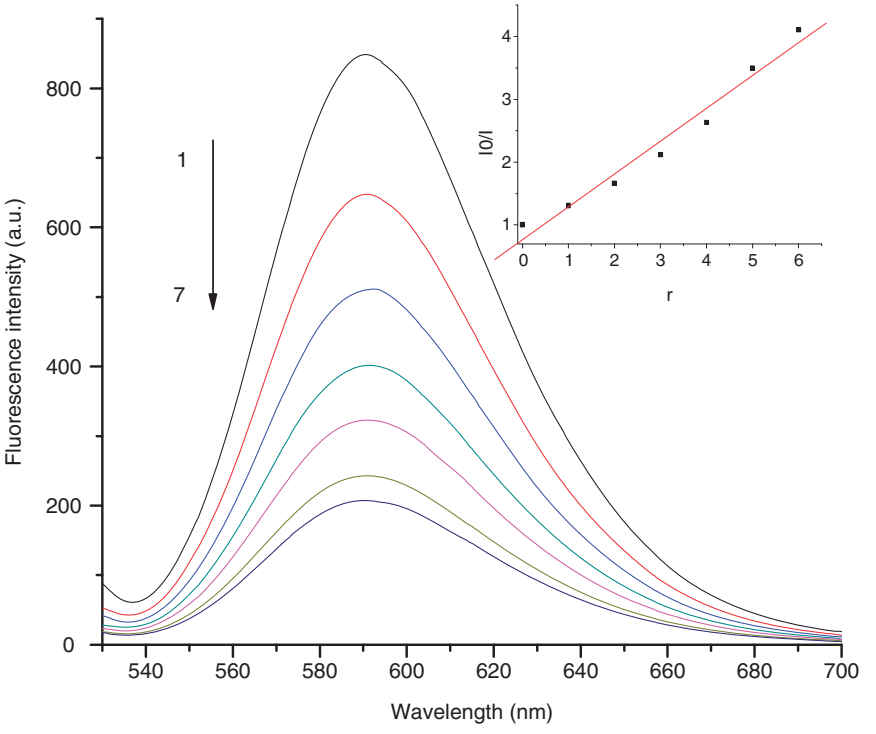

Figure 6. Effects of **2** on the fluorescence spectra of EB-DNA system. $C_{DNA} = 30\,\mu mol\,L^{-1}$; $C_{EB} = 3\,\mu mol\,L^{-1}$; from 1 to 7 $C_{VOL} = 0$, 30, 60, 90, 120, 150, 180 $\mu mol\,L^{-1}$, respectively; Inset: plot of I_0/I *vs.* r ($r = C_{VOL}/C_{DNA}$). $\lambda_{ex} = 258$ nm.

figures 5 and 6, the values of K_{sq} for **1** and **2** can be calculated as 0.16 and 0.52, respectively, indicating stronger interaction between **2** and DNA.

3.6. In vitro *antitumor activity*

Both compounds were screened for *in vitro* antitumor activity against two human tumor cell lines – human lung cancer cell line (A549) and human colon cell line (HCT-8) – at four different concentrations. Comparison of activities between **1** and **2** are shown in the "Supplementary material." Although both show some activity against the two cell lines, for A549, compound **2** exhibits higher activity, while for HCT-8, compound **1** exhibits higher activity. IC_{50} values represent the drug concentration that reduces the mean absorbance at 570 nm to 50% of those in the untreated control wells and it is listed in table 5. Complexes **1** and **2** exhibit similar activity against cisplatin, except that **2** against HCT-8 is a little higher [36, 37].

Analyses of crystal structures of **1** and **2** demonstrate that they have similar coordination geometry. Complex **2** has larger steric hindrance than **1** derived from the ligand, which could result in different inhibition for the same cancer cell. Different cancer cells have different DNA sequences and constituents, etc., and the two organoantimony complexes reported here exhibit different inhibition for A549

Table 5. The values ($\mu g\,m\,L^{-1}$) of IC_{50} for *in vitro* antitumor activity.

Compound	A549	HCT-8
1	9.22	7.46
2	8.56	22.00
Cisplatin	7.0	2.29

and HCT-8. From the fluorescence investigation of DNA, **1** or **2**, and EB, we can conclude preliminarily that the antitumor activities of **1** and **2** are partly due to the interaction of the complexes with DNA of the cancer cell, although there is no obvious linear relationship between the binding ability to DNA and the antitumor activity.

4. Conclusions

This contribution reports two organoantimony derivatives from hydroxamic acids. For **1** hydrogen bonds play an important role in self-assembly of the building block, whilst for **2** weak intermolecular interactions assist in assembling discrete molecules. These examples of organoantimony complexes help explore the structure–activity relationship. There exists stronger interaction via intercalation between **2** and *ct*-DNA than **1** and both exhibit activity against two human tumor cell lines similar to cisplatin, except that of **2** against HCT-8. There is no obvious linear relationship to explain the mechanism of bioactivity.

Supplementary material

Crystallographic data for the structures reported in this article have been deposited with the Cambridge Crystallographic Data Centre: CCDC No. 227143 for **1** and CCDC No. 227144 for **2**. Copies of this information may be obtained free of charge from the director, CCDC, 12 Union Road, Cambridge, CB2EZ, UK (Fax: +44-1223-336033; E-mail: deposit@ccdc.cam.ac.uk or http://www.ccdc.cam.ac.uk).

Acknowledgments

We acknowledge the National Natural Foundation of China (21105042), the National Basic Research Program (2010CB234601), and the Natural Science Foundation of Shandong Province (ZR2011BM007, ZR2010BQ021) for financial support. This work was supported by Shandong "Tai–Shan Scholar Research Fund."

References

[1] D. Copolovici, V.R. Bojan, C.I. Rat, A. Silvestru, H.J. Breunig, C. Silvestru. *Dalton Trans.*, 6410 (2010).
[2] H.J. Breunig, I. Ghesner, M.E. Ghesner, E. Lork. *Inorg. Chem.*, **42**, 1751 (2003).
[3] N.C. Kasuga, K. Onodera, S. Nakano, K. Hayashi, K. Nomiya. *J. Inorg. Biochem.*, **100**, 1176 (2006).
[4] M. Salerno, A. Garnier-Suillero. *Bioinorg. Chem. Appl.*, **1**, 189 (2003).
[5] L. Dawara, R.V. Singh. *J. Coord. Chem.*, **64**, 931 (2011).
[6] R. Agawal, J. Sharma, D. Nandani, A. Batra, Y. Singh. *J. Coord. Chem.*, **64**, 554 (2011).
[7] K. Fan, E. Borden, T. Yi. *J. Interferon Cytokine Res.*, **29**, 451 (2009).
[8] C. Socaciu, A. Bara, C. Silvestru, I. Haiduc. *In Vivo*, **5**, 425 (1991).
[9] E.R.T. Tiekink. *Oncology/Hematology*, **42**, 217 (2002).
[10] L. Dostál, R. Jambor, A. Růžička, R. Jirásko, V. Lochař, L. Beneš, F. de Proft. *Inorg. Chem.*, **48**, 10495 (2009).
[11] A. Gupta, R.K. Sharma, R. Bohra, V.K. Jain, J.E. Drake, M.B. Hursthouse, M.E. Light. *Polyhedron*, **21**, 2387 (2002).
[12] L. Quan, H. Yin, J. Cui, M. Hong, L. Cui, M. Yang, D. Wang. *J. Organom. Chem.*, **694**, 3683 (2009).
[13] H. Yin, L. Quan, L. Li. *Inorg. Chem. Commun.*, **11**, 1121 (2008).
[14] W. Qin, S. Yasuike, N. Kakusawa, Y. Sugawara, M. Kawahata, K. Yamaguchi, J. Kurita. *J. Organomet. Chem.*, **693**, 109 (2008).
[15] Q. Li, M. Fatima, C. Guedes da Silva, A.J.L. Pombeiro. *Chem. Eur. J.*, **10**, 1456 (2004).
[16] X. Shang, J. Wui, Q. Li. Chin. *Chem. Lett.*, **6**, 821 (2006).
[17] Z. Tomkowicz, S. Ostrovsky, H. Müller-Bunz, A.J.H. Eltmimi, M. Rams, D.A. Brown, W. Haase. *Inorg. Chem.*, **47**, 6956 (2008).
[18] I.M. Rio-Echevarria, F.J. White, E.K. Brechin, P.A. Tasker, S.G. Harris. *Chem. Commun.*, 4570 (2008).
[19] J. Schraml. *Appl. Organomet. Chem.*, **14**, 604 (2000).
[20] R. Codd. *Coord. Chem. Rev.*, **252**, 1387 (2008).
[21] B. Kurzak, H. Kozlowski, E. Farkas. *Coord. Chem. Rev.*, **114**, 169 (1992).
[22] B. Chatterjee. *Coord. Chem. Rev.*, **26**, 281 (1978).
[23] G. Wang, Y. Lu, J. Xiao, L. Yu, H. Song, J. Li, J. Cui, R. Wang, F. Ran. *J. Organomet. Chem.*, **690**, 151 (2005).
[24] E. Katsoulakou, M. Tiliakos, G. Papaefstathiou, A. Terzis. *J. Inorg. Biochem.*, **102**, 1397 (2008).
[25] N. Gerasimchuk, T. Maher, P. Durham, K.V. Domasevitch, J. Wilking, A. Mokhir. *Inorg. Chem.*, **46**, 7268 (2007).
[26] J. Dong, L. Li, L. Li, T. Xu, D. Wang. *Chin. J. Chem.*, **29**, 259 (2011).
[27] G. Wang, J. Xiao, L. Yu, J. Li, J. Cui, R. Wang, F. Ran. *J. Organomet. Chem.*, **689**, 1631 (2004).
[28] L. Quan, H. Yin, J. Cui, M. Hong, D. Wang. *J. Organomet. Chem.*, **694**, 3708 (2009).
[29] G. Ferguson, C. Glidewell, D. Lloyd, S. Metcalfe. *J. Chem. Soc. Perkin Trans.*, **2**, 731 (1988).
[30] G. Ferguson, C. Glidewell, B. Kaitner, D. Lloyd, S. Metcalfe. *Acta Crystallogr. Sect. C*, **43**, 824 (1987).
[31] R. Rüther, F. Huber, H. Preut. *J. Organomet. Chem.*, **295**, 21 (1985).
[32] D. Chopra, T.P. Mohan, K.S. Rao, T.N.G. Row. *CrystEngComm*, **7**, 374 (2005).
[33] M. Nishio. *CrystEngComm*, **6**, 130 (2004).
[34] C. Ma, Q. Zhang, R. Zhang, D. Wang. *Chem. Eur. J.*, **12**, 420 (2006).
[35] B.C. Baguley, M. Le Bret. *Biochemistry*, **23**, 937 (1984).
[36] J.J. Wilson, S.J. Lippard. *Inorg. Chem.*, **50**, 3103 (2011).
[37] G. Xu, Z. Yan, N. Wang, Z. Liu. *Eur. J. Med. Chem.*, **46**, 356 (2011).